CRS data imaging: a case study for basin reevaluation

L. Leite, Z. Heilmann, I. Koglin, M. von Steht, and J. Mann

email: *lwbleite@ufpa.br*

keywords: *Preprocessing, CRS stack, tomography, migration.*

ABSTRACT

A real land data set of the Takutu basin (Brazil) was processed as an example not for comparison with other processing packages, but to demonstrate once more the high potential of data-driven Common-Reflection-Surface (CRS) stack-based imaging methods. The aim of this ongoing project is to establish a workflow for basin reevaluation for oil play. Based on the CRS attributes obtained during the CRS stacking process, the determination of a smooth macrovelocity model via tomographic inversion was conducted, followed by pre- and/or poststack depth migration.

It will be shown that both, pre- and poststack depth migration benefit from this approach. Other CRS-stack based processing steps which could be added to this workflow are, e. g., residual static corrections, limited-aperture migration based on the estimated projected Fresnel zone, determination of the geometrical spreading factor, and analysis of amplitude variation versus offset in the time domain using approximate common-reflection-point trajectories calculated from CRS attributes.

Geological interpretation should be carried out mainly on the basis of zero-offset (ZO) and migrated sections, being important that all maps have the proper scale, axis exaggeration and size. From details, an anticline structure and faults can be mapped, where plays of horsts, grabens and rollovers are indicated. Nevertheless, the basement cannot easily be traced. Especially, the right part of the section needs more processing studies.

INTRODUCTION

This report is centred on results obtained for the land seismic data of the Takutu graben, where we used the processing and imaging workflow and results of the Rhein graben seismic data presented in Heilmann et al. (2003) as reference. The latter publication serves, together with Mann et al. (2004), as the basic references on the CRS stack data-driven imaging approach for this report. Considering that most reflection seismic surveys are subject to proprietary laws, our intention is to have data accessible to academic projects for basin reevaluation.

The presented Takutu data set was acquired by Petrobras (Takutu Basin, Rondônia, Brazil) for petroleum exploration. The data is free for use on university research and it was obtained from Agência Nacional do Petróleo (ANP), Brazil. The goal here is to support academic projects that can deal with basin reevaluation based on seismic reprocessing. The software used is non-commercial and developed, in the spirit of continuous cooperation with the Geophysics Department of the Federal University of Pará, Brazil, by the WIT Consortium group in Karlsruhe, Germany. This data set is offered in the form of non-processed field records, therefore a complete pre-processing stage was necessary and described in the sequel.

The Takutu basin, following the description by Eiras and Kinoshita (1990), is classified as a Mesozoic intracontinental rift, oriented NE-SW and approximately 300 km long and 40 km wide. It was developed in the central part of the Guyana shield and located at the border Brazil and Guyana. The rift is filled with sediments ranging from the Jurassic to the Quaternary and composed of two asymmetrical half-grabens: The SW part dips southeasterly and the NE part dips northwesterly.

The structural scenario of the Takutu basin features horsts, grabens, anticlines, synclines, flower structures,

and dip inversions (rollovers). Transcurrent faulting is considered to have reactivated local features that were developed in the rift stage. The stratigraphical scenario of the Takutu basin is divided into four depositional sequences that reflect the geological evolution of the area. The first basal sequence is represented by the volcanic Apoteri formation and by the shaly Manari formation, both related to the pre-rift phase. The second sequence is represented by the evaporitic Pirara formation and relates to the stage of maximum stretching in the rift phase. The third sequence is represented by the sands and conglomerates of the Tacutu and Tucano formations and are interpreted to correspond to the continuous decrease in stretching. The fourth sequence is represented by the lateritic and alluvium of the Boa Vista and North Savannas formations.
Continuing with Eiras and Kinoshita (1990), the conclusions for the model of the Takutu basin were formally based on the interpretation of the conventional processed seismic data, seismic reprocessing, seismic stratigraphy, surface geology, drilled wells, geochronology, and geochemistry. Several structural styles were considered for the basin in focus and the most attractive were deltaic fan-shaped, compressional inversions, internal horst highs, and dip reversals. Our intention at this moment is not to trace new evidences for the structural scenario for the Takutu basin, what may follow with the advance of the studies with more systematically processed data completing a full block, followed by an enlarged work-group for a proper geological interpretation.

The workflow for reference was the one for the data sets of the Rhein graben area acquired by the HotRock Company with the aim to obtain a structural image of relevant structures for a projected geothermal power plant. A power plant is based on boreholes for production and re-injection of thermal water at a depth of ≈ 2.5 km, where a strong fractured horizon of hot-water saturated shell limestone is to be located. The production rate depends mainly on the degree of fracturing of a target horizon and a detailed knowledge of the subsurface structure is necessary. A standard preprocessing was applied to the Rhein graben data set, followed by an imaging sequence consisting of: (1) normal-moveout (NMO) correction stack; (2) dip-moveout (DMO) correction stack; (3) Finite difference (FD) time migration; and (4) a time-to-depth conversion using macrovelocity models based on stacking velocity sections. Complementary to this standard processing, the main steps of the CRS-stack-based seismic imaging workflow were carried out. Also, additional tasks, such as residual static corrections, true-amplitude migration, and amplitude variation with offset (AVO) analysis may follow in the course of further research collaboration.
The CRS-stack-based seismic imaging workflow is presented in Figure 1. A fundamental point for good CRS stack results is the preprocessing of the multicoverage seismic reflection data. The preprocessing was performed in several steps beginning with the geometry setup and muting of bad shot and receiver gathers followed by F-filtering, F-K-filtering, amplitude correction, and deconvolution. Since there were no significant changes in elevation, field static correction were omitted.
It has been reported in the recent 5 years by several case studies (Gierse et al., 2003) that CRS stack produces reliable stack sections with high resolution and signal-to-noise (S/N) ratio. A set of physically interpretable stacking parameters is determined as a result of the data-driven stacking process. These kinematic wavefield attributes obtained by the CRS stack are important because they can be applied to resolve a number of dynamic and kinematic problems. CRS-stack-based seismic imaging can make use of these extended possibilities in further processing, e.g., to determine a smooth macro-velocity model or to consider rugged top-surface topography. Besides the 2-D implementation used in this study also a 3-D implementation, including parallel processing technology, is available.

PREPROCESSING

This section is mainly concerned with the tasks related to the Takutu original non-processed field data. After a previous analysis, the selected line for processing was the one numbered 204-239 and it has the following survey information: date of acquisition 1986; direction NW-SE; length of 31.5km; 631 shot points; 4ms of time sampling interval; 50m spacing of shot points and stations; charges of 0.9kg at 2m depth distributed as L-3x2/25m. The receiver array distribution from left to right starts with a part right-unilateral 0-48; the second part is split-spread symmetrical 48-48; the third part is split-spread asymmetrical 76-20; and the fourth part is a left-unilateral 76-0. Similar procedures can be carried out for all the lines of the two seismic blocks (numbered 50 and 204) of the Takutu graben. As before

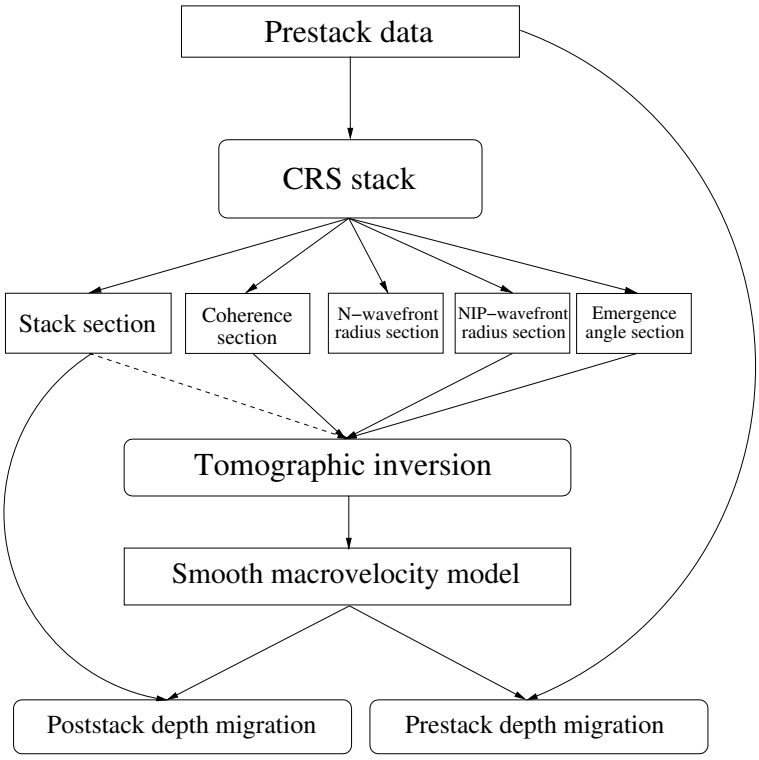

Figure 1: The CRS-stack-based seismic imaging workflow.

mentioned, the topography of the terrain is very smooth to almost flat so that elevation statics were omitted.

The preprocessing steps were performed with the Seismic Un*x (SU) package of the Colorado School of Mines (Cohen and Stockwell, 2000). The SU data format is standard in almost every CRS imaging tool. To facilitate an easy reproduction of the results, the tasks performed were organised in a so-called Makefile. It severs as important reference information, as the further CRS imaging process is highly dependent on the preprocessing. In our case, it consisted mainly of three parts: (1) Geometry setting; (2) Muting of bad traces; and (3) F and F-K filtering. Besides these main parts, the workflow was subdivided into minor steps given below.

1. Converting data format

1.1 Convert data from SEGY to SU and look at content of headers

2. Setting geometry

2.1. Set record number and trace number
2.2. Remove non-existing files reported on the field report
2.3. Set shot point coordinates
2.4. Set receiver point coordinates
2.5. Concatenate all shot gathers into one file
2.6. Set offset values
2.7. Set trace number within each CDP gather
2.8. Sort traces by CDP and offset

3. Discriminating bad traces

3.1. Detect and zero out bad common-receiver (CR) gathers
3.2. Detect and zero out bad common-source (CS) gathers
3.3. Detect and zero out remaining bad traces

4. Muting

4.1. Select and mute top part of CS gathers (surface waves, refractions and noise)
4.2. Select and mute corrupted parts and coherent noise where possible

5. Filtering

5.1. Check dataset and apply trapezoidal bandpass filter: f=10,20,40,50 Hz
5.2. Check CS gathers and apply appropriate dip filters
5.3. Repeat muting

6. Trace balancing

6.1. Apply automatic gain control (AGC) with Gaussian window of 1s

As a first observation about the original Takutu seismic land data, the line 204-239 has many noisy sections. For this reason, several shot and receiver gathers were initially completely muted. As a result of visual analysis of all shot gathers, again several single traces had to be zeroed due to the high noise level like spikes and sensor wandering. Afterwards, several band-pass filters with trapezoidal form were experimented and the decision was for adopting the case with corners 10-20-40-50 Hz. The F-K velocity dependent filter was used to further emphasise the cutting of high and low frequent noise, as surface waves and critically refracted waves. The decision for adopting the filter parameters was based on the trace gathers analysis through the spectrum and preliminary stack results, reinforcing the importance of the pre-processing stage on the CRS stack results. Also, it should be clear that, intentionally at the current stage, no techniques as, e.g., radon filtering or ghost deconvolution were carried out on this data. Therefore, increased results on stacking, tomography and migration might be obtained after inclusion of such advanced pre-processing techniques.

CRS-STACK-BASED IMAGING

For the visualisation of the CRS attributes (see, e.g., Mann, 2002), the coherence section should be used to mask out locations with very low coherence, considering that such locations are not expected to be associated with reliable attributes. For these preliminary results, this step as well as the calculation of additional output sections as, e.g., the optimized NMO velocity section and the geometrical spreading section was omitted. The obtained sections of kinematic CRS wavefield attributes, as indicated in Figure 1, are the following:

- a section containing the emergence angle of the central ray with respect to the measurement-surface normal.
- a section containing the radius of the normal-incidence-point (NIP) wavefront as observed at the emergence point of the central ray. The NIP wave focuses at that point of the reflector, where the respective central ray is reflected, i. e., at the NIP.
- a section containing the curvature of the normal wavefront which can be observed at the emergence point of the central ray due to an exploding reflector element at the NIP.

It is evident that a single display cannot emphasise all objective parts of the whole survey; therefore, a prominent display was selected. Figure 2 displays the coherence panel that serves to indicate the fit between the determined CRS stacking operators and the reflection events. Figure 3 displays the number of traces used on the CRS stack process. It is clearly visible that there are zones of lower trace density.

This laterally variable trace density corresponds to the changing acquisition geometry along the line and to missing shotpoints. Figure 4 displays the radius of curvature of the normal-incidence-point wave (R_{NIP}). Figure 5 displays the radius of curvature of the normal-wave (R_N). Figure 6 displays the emergence angle of the central ray (β). This complete set of CRS wavefield attributes allows to estimate the size of the projected first Fresnel zone. This is done by comparing the traveltime of the actual reflection event with the traveltime of its associated diffraction event (characterised by the identity $R_N = R_{NIP}$). The locations where these events differ by half the temporal wavelet length define the extension of the projected first Fresnel zone, and, thus, the optimum aperture to apply the attribute search and the stack. In addition to the stack performed in the user defined aperture, a second stack is performed within the projected Fresnel zone, only. Figure 7 displays the simulated non-Fresnel CRS ZO panel. Figure 8 displays the simulated Fresnel CRS ZO panel. Figure 9 displays a typical near-offset gather for a direct use in the analysis of ZO section in interpreting underlying reflectors. However, we can observe the difficulties in doing so. Figure 10 displays a selected window of the ZO Fresnel stack panel for detailed analysis in interpreting underlying reflectors. Figure 11 displays the same window now used for the automatic picking of CRS attributes needed by the tomographic inversion. The time samples where CRS attributes have finally been picked (after some editing) are marked by green crosses. Figure 12 displays the velocity model distribution obtained by the tomographic inversion and it serves as input for the migration process. Figures 13 and 14 display the prestack and poststack depth migration panels, respectively.

The section depicted in Figure 10 shows that part of the ZO section which was used for the tomographic inversion and migration. There, a prominent reflector dips from ≈ 0.5 s (left) to ≈ 1.5 s (right). The most prominent anticline structure is on the left side between ≈ 2.0 km and ≈ 6.0 km. Although the preliminary set of CRS attribute sections, at first glance, seems to be without good and clear correlative information, the simulated zero offset sections show rather surprising correlated patterns in the panel.
A tomographical inversion based on the kinematic NIP wavefront attributes, as developed by Duveneck (2002), was carried out to obtain a data consistent smooth macrovelocity model for depth imaging of time-domain pre- and/or poststack data. This method is based on the description of the smooth macrovelocity model by two-dimensional B-splines. It performs a simultaneous fit to all data points during every iteration, in a least squares sense. Thus a simultaneous update of all model parameters is possible after each iteration. In this case study, about several hundreds of ZO samples together with the associated attribute values were picked to achieve the best resolution possible. Automatic picking was carried out using a module based on the coherence associated with the ZO samples. The picked data, as shown in Figure 11, was edited using several criteria to discriminate outliers and attributes related to multiples, before the tomographic inversion process was applied. The obtained macrovelocity model is displayed in Figure 12. During the first iterations the velocity models obtained changed rapidly, starting from a simple gradient model. However, after four or five iterations they got more and more similar, ending up with the displayed model after ten iterations.

A prestack depth migration (Hertweck and Jäger, 2002; Jäger and Hertweck, 2002) based on the macrovelocity model, obtained in the tomographic inversion, was applied to the prestack data of both profiles, where the kinematic Green's function were calculated by means of an eikonal solver. The resulting depth-migrated prestack data was first muted to avoid excessive pulse stretch for shallow reflectors and then stacked in offset direction in order to obtain the depth-migrated images displayed in Figures 13 and 14. Both sections do not show the same amount of structures, as in the stacked sections. However, these results are preliminary, and do by far not tap the full potential of CRS imaging. Therefore they cannot be compared to results of standard processing, where a sophisticated and very laborious preprocessing and NMO/DMO/stack process was applied, using additional information (as refraction seismics or borehole data) which was not yet considered for these preliminary results.
Nevertheless, even the results obtained so far by CRS-stack-based imaging show to be consistent for the major structural trends and it is expected that the depth location of the reflectors are more reliable. Comparison of the presented results with existing borehole data and other geological and geophysical information available for the investigated area (Eiras and Kinoshita (1990)) shows agreement.

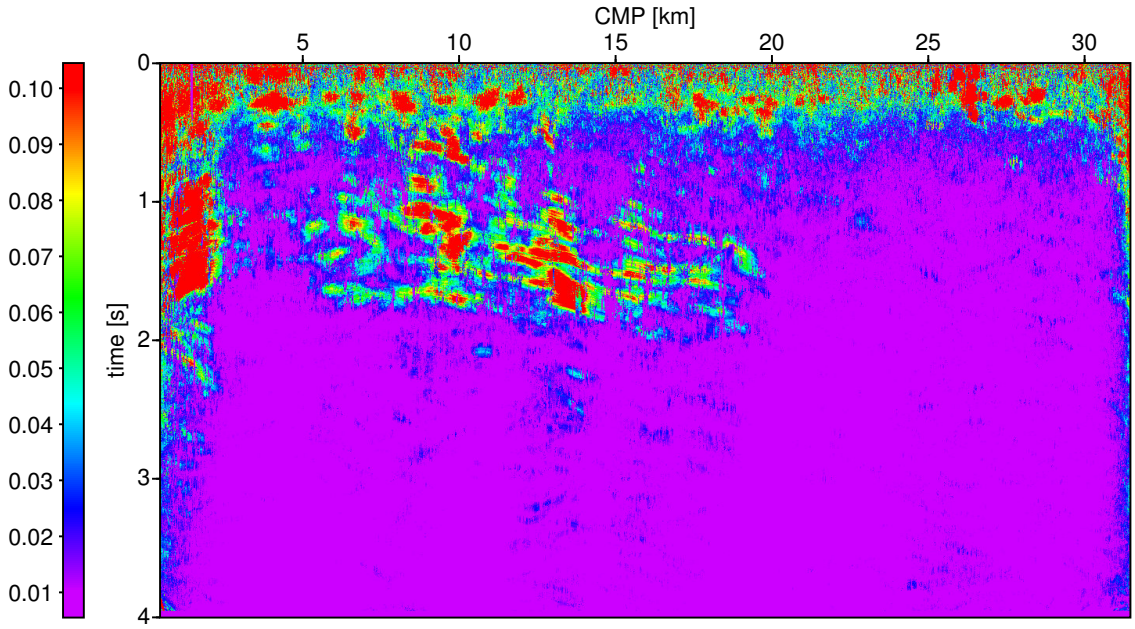

Figure 2: Coherence panel for line Takutu 204-239.

As a complementary or alternative step of the CRS-stack-based imaging workflow, a poststack depth migration was carried out for the profile. Input for the poststack depth migration are the CRS-stacked section and the macrovelocity model derived from the CRS attributes via tomography. In general, poststack depth migration can be advantageous in cases where the determination of a sufficiently accurate macrovelocity model is difficult and/or the signal-to-noise ratio is poor. As both of these conditions might be met in the case discussed here, where the data quality is considered to be low and therefore a macrovelocity model, determined fully data-driven, may not be very reliable. For these preliminary results, prestack depth migration cannot fully compete with the poststack depth migration in view of resolution and image quality. However, there are also regions, especially at greater depths, where some details are better resolved by the prestack depth migration. As a summary, prestack and poststack depth-migrated results can provide complementary information for questions related to a seismic reevaluation, in the sense that both migrations serve as a double check on the previously obtained model.

CONCLUSIONS

Geological interpretation should be carried out mainly on the basis of Figures 7, 8, and 10, together with the details given in Figures 13 and 14, being important that all maps have the proper scale, axis exaggeration and size. From details of Figure 10, a long anticline structure and several faults, where plays of horsts, grabens, and rollovers are indicated, can be mapped . Nevertheless, from Figures 7 and 8, the basement cannot be easily traced. Especially, the right part of the section needs more processing studies.
Here, a standard processing sequence with commercial software was not carried out. The presented study is not intended to compare softwares, but to compare geological targets represented by the Takutu graben for oil exploration, and by the Rhein graben for geothermal exploration.
The coherence sections served to indicate the fit between the determined CRS stacking operators and the reflection events in the prestack data. The overall Takutu seismic image quality is quite low compared to the high quality of the Rhein seismic image. In both cases, the results obtained by CRS revealed good signal-to-noise ratio and reflector continuity.

The quality of the Takutu seismic data is a limitation in enhancing different parts of imaging the selected line. The ideal is still to process other lines completing a full block to demonstrate the applicability of the CRS-stack-based imaging basin reevaluation project. The CRS formalism is proposed because the applied methodology can provide good basis for the geological interpretation, but it would be important to conduct

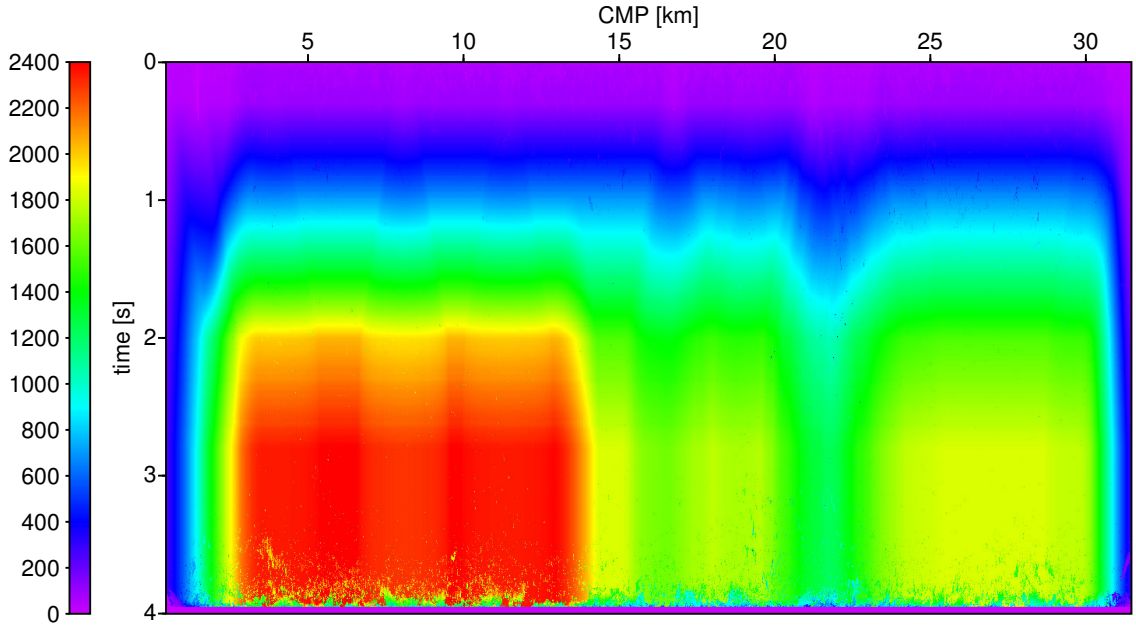

Figure 3: Density of traces for line Takutu 204-239.

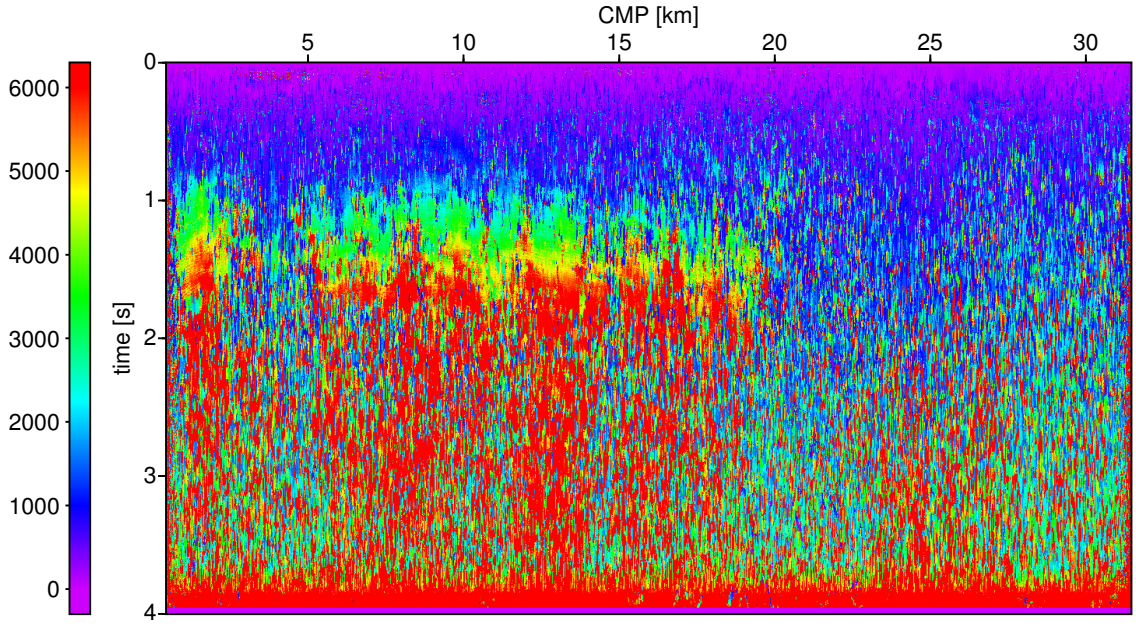

Figure 4: Radius of curvature [m] of normal incidence wave (R_{NIP}) for line Takutu 204-239.

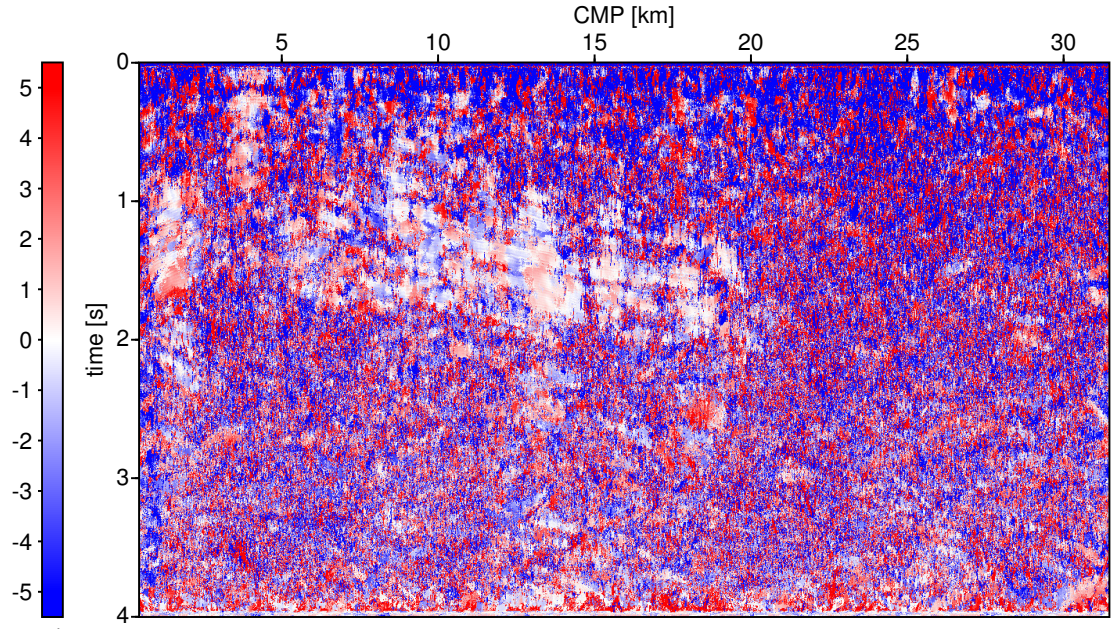

Figure 5: Curvature [1/km] of normal wave $(1/R_N)$ for line Takutu 204-239.

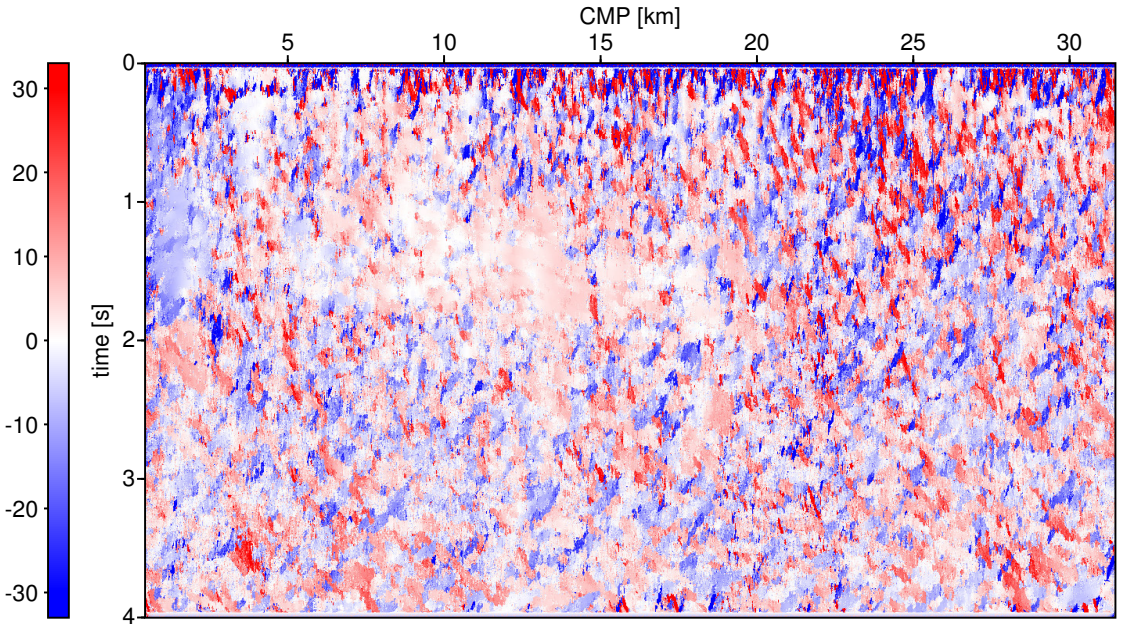

Figure 6: Emergence angle [°] of central ray (β) for line Takutu 204-239.

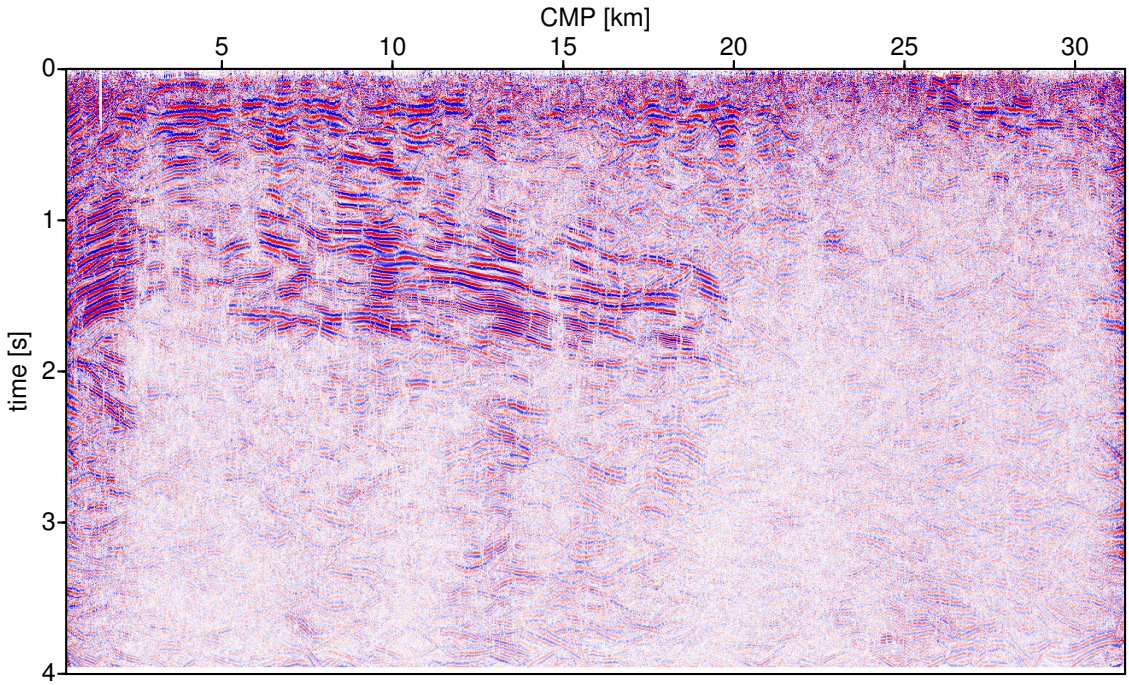

Figure 7: Takutu optimized CRS non-Fresnel stack zero-offset panel for line 204-239.

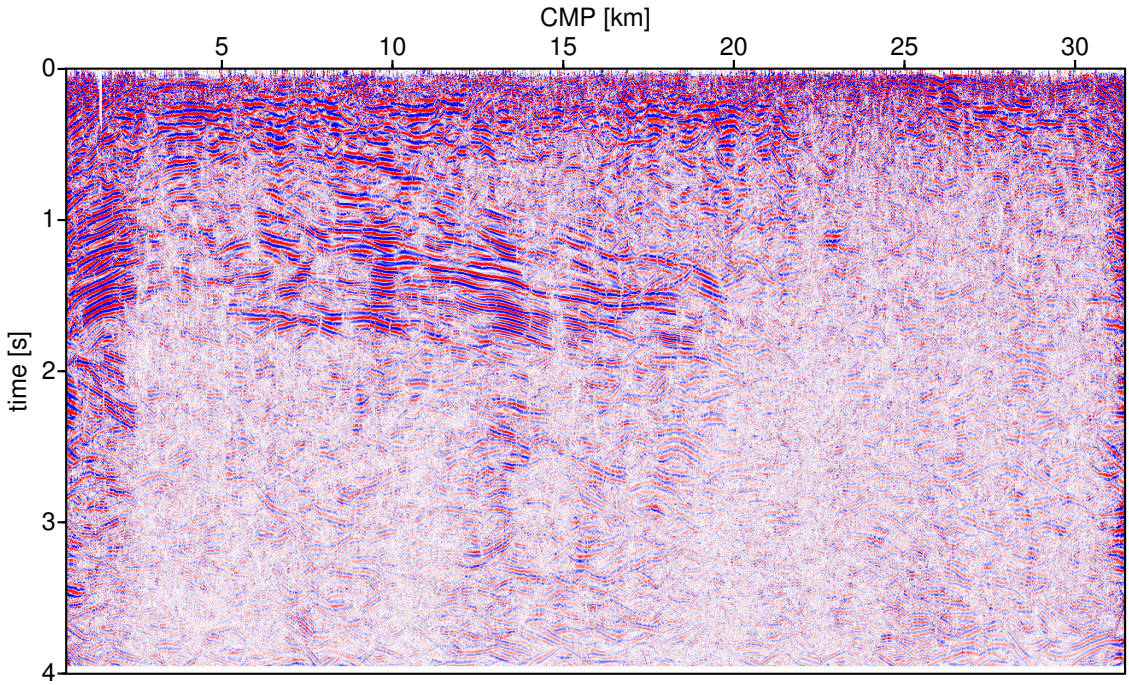

Figure 8: Takutu CRS Fresnel stack zero-offset panel for line 204-239.

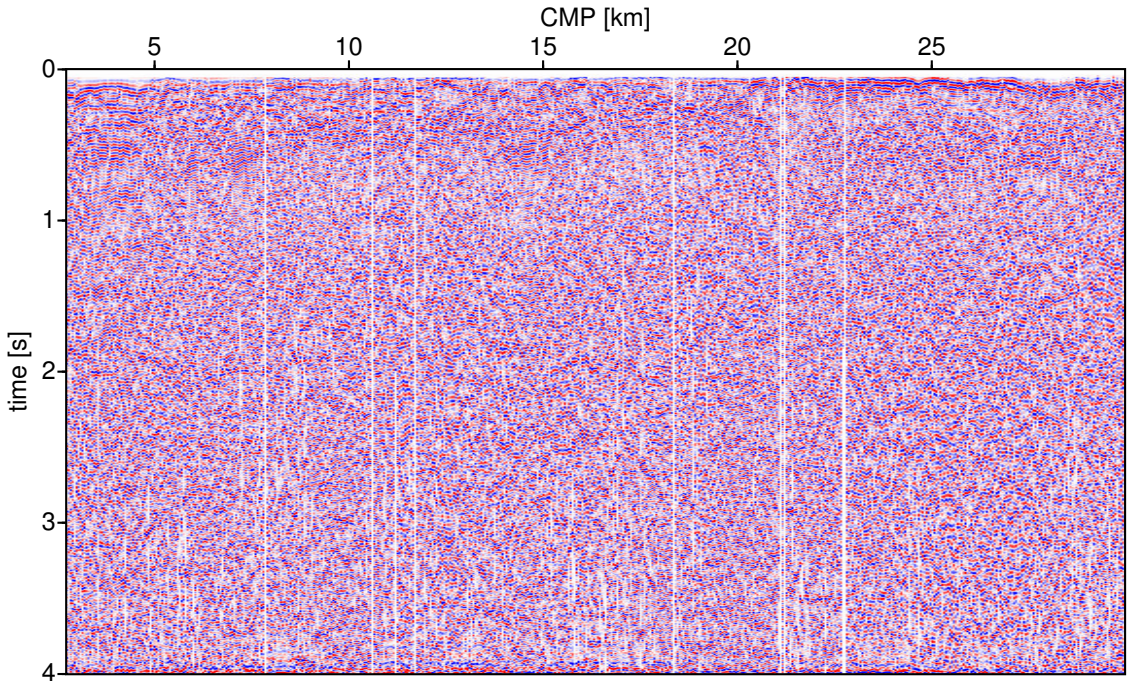

Figure 9: Selected near-offset gather (-100 m) for comparison with the ZO section.

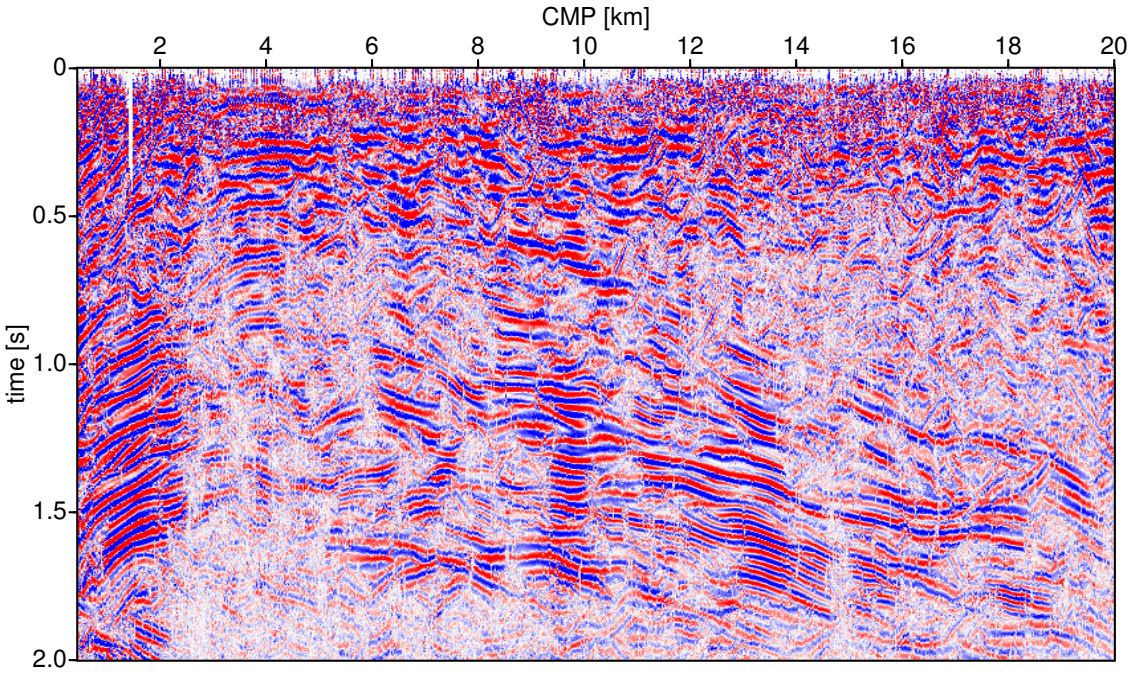

Figure 10: Subsection of the optimized CRS Fresnel stack zero-offset panel used for the tomography and migration imaging.

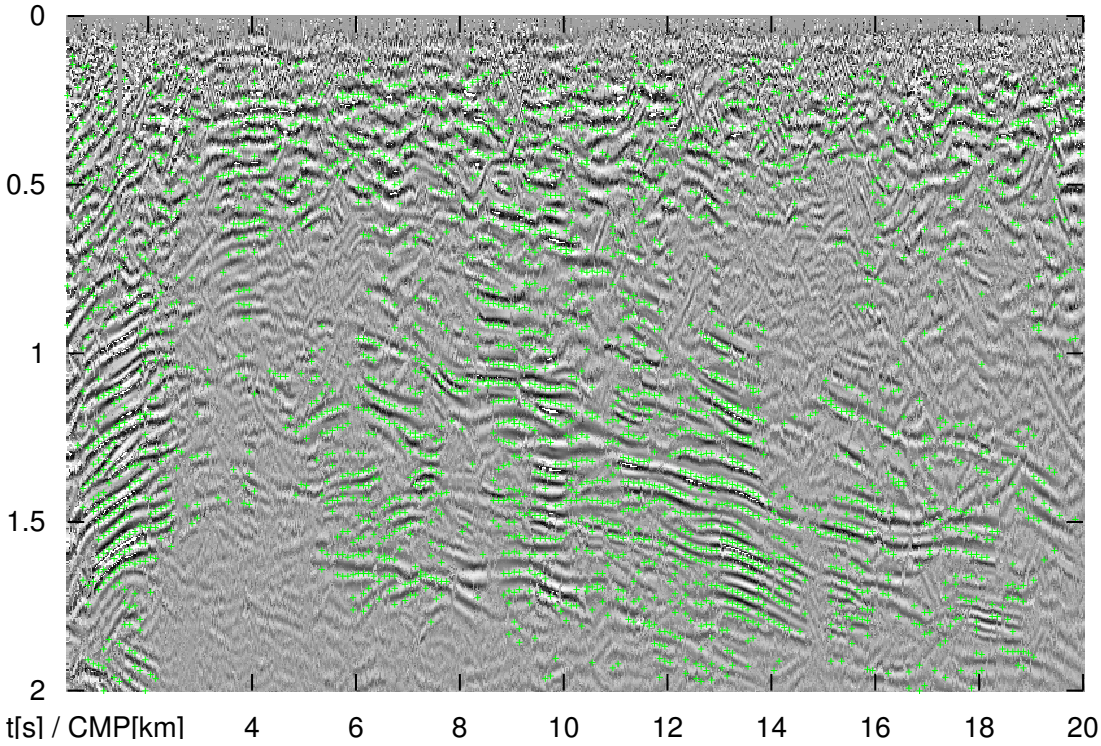

Figure 11: ZO locations of picked CRS attribute values used for tomographic inversion shown as green crosses.

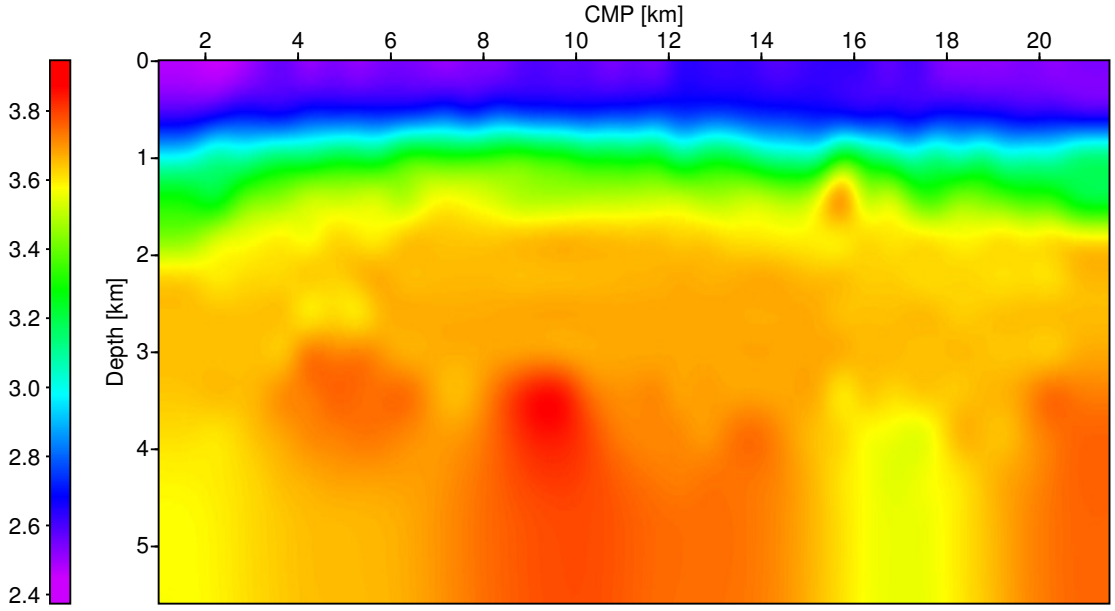

Figure 12: Selected macrovelocity model [km/s] obtained by CRS attribute-based tomographic inversion.

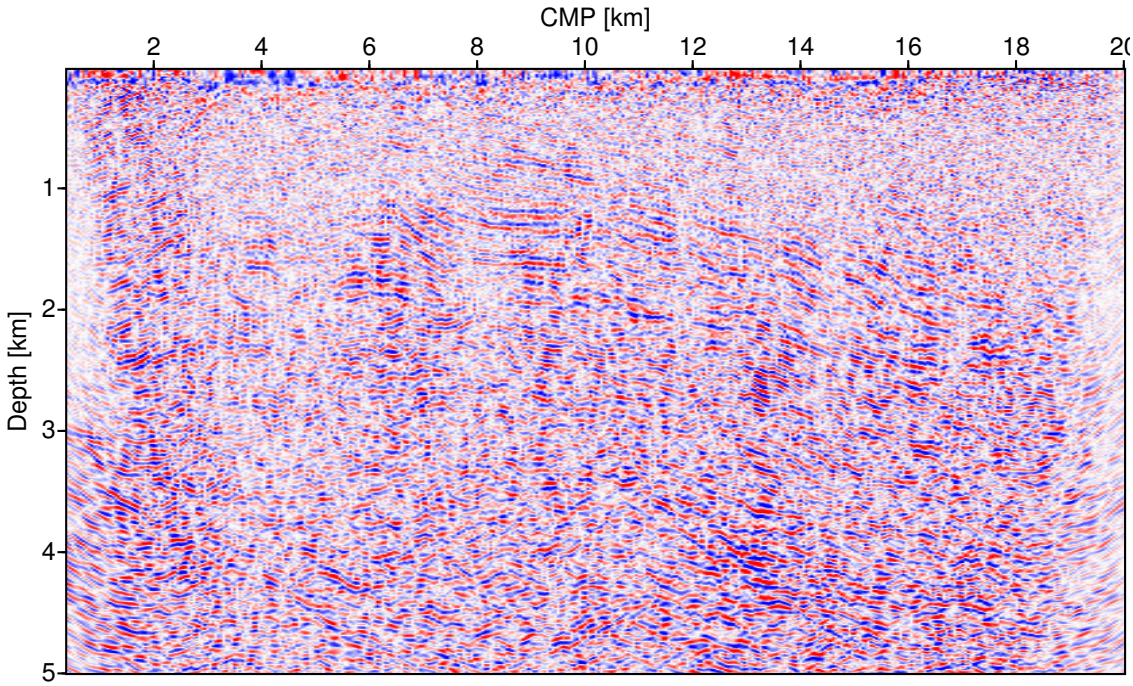

Figure 13: Preliminary prestack depth migration (PreSDM) result.

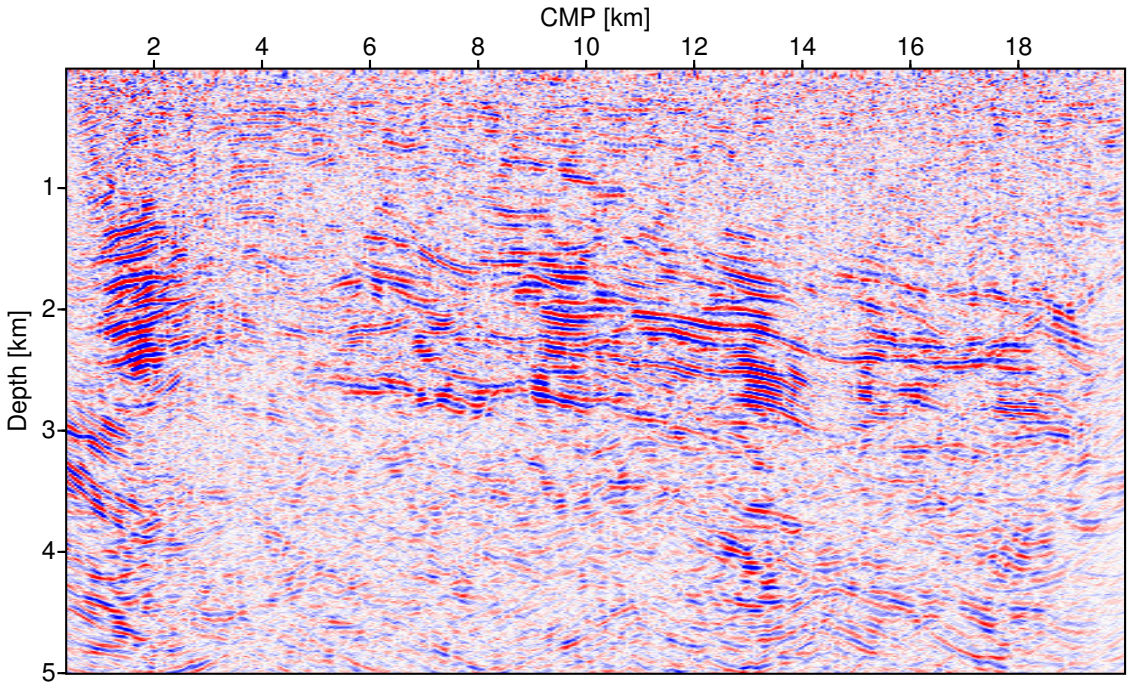

Figure 14: Preliminary poststack depth migration (PostSDM) result.

the velocity analysis more closely in order to check for possible structural inversion on the stack part. It is clear that as the quality of the seismic data becomes high, it provides an ideal basis to apply and enhance the different parts of the seismic imaging software and to demonstrate its practical applicability by means of a real data example. The obtained results provide good grounds for giving continuity to the Takutu seismic data reprocessing, geological reinterpretation, and for a hopefully successful drilling.

This example serves to reinforce our perspectives and intentions on research collaboration between University and Industry to provide foundation for applied seismics.

ACKNOWLEDGEMENT

The authors would like to thank the Brasilian institutions UFPa (Universidade Federal do Pará), FINEP (Financiadora de Estudos e Projetos, ANP (Agência Nacional do Petroleo), PETROBRAS (Petróleo Brasileiro S/A), and all sponsors of the WIT consortium for research support. Otherwise the presented project, i.e., Exploration Risk Net (Rêde 01/03, Rêde Risco Exploratório, FINEP 22.01.0763.00), would have been impossible to be carried out. The thanks are also extended to the WIT Administration. Finally we like to thank Miriam Spinner, and Tilman Klüver for provided help and fruitful collaboration.

REFERENCES

Cohen, J. K. and Stockwell, J. J. W. (2000). *CWP/SU: Seismic Unix Release 34: a free package for seismic research and processing*. Center for Wave Phenomena, Colorado School of Mines.

Duveneck, E. (2002). Tomographic velocity model inversion with CRS attributes. *Annual WIT report*, pages 92–106.

Eiras, J. and Kinoshita, E. (1990). Geology and Petroleum Perspectives of the Takutu Basin. *In: Raja Gabaglia, G.P. and Milani, E.J. Origin and Evolution of Sedimentary Basins. (In Portuguese)*, pages 197–220.

Gierse, G., Pruessmann, J., Laggiard, E., Boennemann, C., and Meyer, H. (2003). Improved imaging of 3D marine seismic data from offshore Costa Rica with CRS processing. *First Break*, 21(12):45–49.

Heilmann, Z., Mann, J., Duveneck, E., and Hertweck, T. (2003). CRS-stack-based seismic imaging - a real data example. *Annual WIT report*, pages 150–163.

Hertweck, T. and Jäger, C. (2002). Short note: various aspects of Kirchhoff migration. *Annual WIT report*, pages 133–142.

Jäger, C. and Hertweck, T. (2002). Using Uni3D version v0.23: a manual. *Annual WIT report*, pages 143–150.

Mann, J. (2002). *Extensions and applications of the Common-Reflection-Surface stack method*. Logos Verlag, Berlin.

Mann, J., Duveneck, E., Bergler, S., and Hubral, P. (2004). The Common-Reflection-Surface (CRS) stack – a data-driven space-time adaptive seismic reflection imaging procedure. *In Klemm, R., editor, Applications of Space-Time Adaptive Processing, chapter VIII.4*.